Directed Synthesis of Silica Nanoparticles on Micropatterned Hydrogel Templates Tethered with Poly(ethyleneimine)

Jamie Ford and Shu Yang*

Department of Materials Science and Engineering, University of Pennsylvania, 3231 Walnut Street, Philadelphia, Pennsylvania 19104

Received June 12, 2007. Revised Manuscript Received August 16, 2007

Poly(ethyleneimine) (PEI) was covalently grafted to hydrogel films of poly(2-hydroxyethyl methacrylate-*co*-acrylic acid) (PHEMA-*co*-PAA) to direct the growth of silica nanoparticles from a sol−gel reaction at room temperature and pH 5. The deposition was found to be site-specific, and the thickness and morphology of the SiO_2 nanoparticles was controlled by PEI molecular weight and exposure time to $Si(OH)_4$. Our results suggest that PEI attacked the ethyl ester groups on PHEMA, resulting in complete penetration of PEI chains and deposition of silica nanoparticles throughout the film. After pyrolysis at 500 °C, a faithful SiO_2 replica of the patterned polymer template was obtained. We believe that the synthetic route described here can be extended to the synthesis and patterning of a wide range of inorganic oxides, including TiO_2, ZnO, and V_2O_5 with controlled hierarchical organization.

Introduction

Inorganic materials with complex micro- and nanostructures are important to many applications, including catalysis, lightweight structural materials, biomedical devices, photonics, phononics, and photovoltaics. Control of their structures, however, is nontrivial and mainly achieved by top-down fabrication methods, such as chemical vapor deposition and laborious lithography/etching processes. In contrast, biomineralization is a bottom-up process and biominerals, such as diatom exosekeltons, often exhibit hierarchical organization ranging from the nanometer to macroscopic length scales and possess remarkable optical, structural, and mechanical properties.[1] Therefore, biomineralization offers inspiration to develop new synthetic routes to create novel hybrid materials.

The formation of biominerals is genetically controlled and optimized locally by specialized biomacromolecules (proteins or polypeptides),[2] which act as structured organic matrices and soluble additives that are actively involved in the sequestration, scaffolding, and chaperoning of inorganic precursors. In addition, biomineralization occurs at ambient temperatures and physiological pH in aqueous solution as opposed to the traditional "heat and beat" synthesis of inorganic materials.

Diatoms, for example, are eukaryotic algae that grow intricate silica exoskeletons.[3] Specialized vesicles in the cell wall trap silicic acid, where a class of proteins, known as sillafins or silacateins, catalyzes the condensation and hydrolysis into silica through a sol−gel process.[4−10] The hierarchical bottom-up deposition of the silica exoskeleton ranges from the nanoscale to the microscale control; the morphology of the proteins and buffer conditions dictate the deposition of silica nanoparticles that are constrained on the microscale by the morphology and location of vesicles in the cell wall. Studies into the mechanism of protein-catalyzed silica formation suggest that the driving force is dominated by electrostatic interactions between positively charged amines and negatively charged species of $Si(OH)_4$ or SiO_2 in solution. Initial clustering of $Si(OH)_3O^-$ ions near NH_4^+ groups facilitate the hydrolysis and condensation of SiO_2 nanoparticles around the polyamine template,[11] which in turn directs the spatial deposition of silica.[5−10]

A number of biomineralization principles have been borrowed in the design and synthesis of silica nanocomposites using polymers as templates. For example, a range of synthetic polyamines, including poly(phenylene vinylene), poly(allylamine), poly(L-arginine), poly(L-lysine), and poly(ethyleneimine) (PEI), have been used to deposit silica nanoparticles with a wide variety of shapes, including platelets, spheres, and rods, in solution.[12−23] In solution, the

* To whom correspondence should be addressed. Tel: (215) 898-9645. Fax: (215) 573-2128. E-mail: shuyang@seas.upenn.edu.

(1) Aizenberg, J. *Adv. Mater.* **2004**, *16* (15), 1295.
(2) Meldrum, F. C. *Int. Mater. Rev.* **2003**, *48* (3), 187.
(3) Chiappino, M. L.; Volcani, B. E. *Protoplasma* **1977**, *93*, 205.
(4) Cha, J. N.; Shimizu, K.; Zhou, Y.; Christiansen, S. C.; Chmelka, B. F.; Stucky, G. D.; Morse, D. E. *Proc. Natl. Acad. Sci. U.S.A.* **1999**, *96*, 361.
(5) Kröger, N.; Deutzmann, R.; Sumper, M. *Science* **1999**, *286*, 1129.
(6) Kröger, N.; Deutzmann, R.; Bergsdorf, C.; Sumper, M. *Proc. Natl. Acad. Sci. U.S.A.* **2000**, *97*, 14133.
(7) Sumper, M. *Science* **2002**, *295*, 2430.
(8) Sumper, M.; Kröger, N. *J. Mater. Chem.* **2004**, *14*, 2059.
(9) Sumper, M. *Angew. Chem., Int. Ed.* **2004**, *43*, 2251.
(10) Sumper, M.; Brunner, E.; Lehmann, G. *FEBS Lett.* **2005**, *579*, 3765.
(11) Coradin, T.; Durupthy, O.; Livage, J. *Langmuir* **2002**, *18*, 2331.
(12) Patwardhan, S. V.; Mukherjee, N.; Clarson, S. J. *Silicon Chem.* **2002**, *1*, 47.
(13) Patwardhan, S. V.; Clarson, S. J. *J. Inorg. Organomet. Polym.* **2002**, *12*, 109.
(14) Patwardhan, S. V.; Clarson, S. J. *Silicon Chem.* **2002**, *1*, 207.
(15) Patwardhan, S. V.; Clarson, S. J. *Polym. Bull.* **2002**, *48*, 367.
(16) Patwardhan, S. V.; Clarson, S. J. *J. Inorg. Organomet. Polym.* **2003**, *13*, 193.
(17) Patwardhan, S. V.; Clarson, S. J. *Mater. Sci. Eng., C* **2003**, *23*, 495.
(18) Patwardhan, S. V.; Clarson, S. J. *J. Inorg. Organomet. Polym.* **2003**, *13*, 49.
(19) Patwardhan, S. V.; Clarson, S. J.; Perry, C. C. *Chem. Commun.* **2005**, 113.
(20) Mizutani, T.; Nagase, H.; Fujiwara, N.; Ogoshi, H. *Bull. Chem. Soc. Jpn.* **1998**, *71*, 2017.

10.1021/cm071566q CCC: $37.00
Published on Web 10/11/2007

chemistry, composition, structure, molecular weight, and architecture of the polyamine combined with the buffer conditions of the sol−gel precursors determine the morphology of the resulting silica nanoparticles.[12−23] Moving the synthesis from solution to a patterned, solid substrate expands the control we have over the location and shape of the deposited inorganic materials over multiple length scales. Fabrication strategies, such as holographic patterning,[24] direct-write assembly,[25] electrostatic deposition,[26] and surface-initiated polymerization,[27] have been demonstrated to create patterned films of polyamines or polypeptides that serve as templates that direct silica deposition on the microscale. However, questions remain of how to achieve both nanoscale and microscale control while maintaining the patterned film integrity during the sol−gel process, the location of silica particles deposited in the polymer template (throughout the film or only on the surface), and how the morphology of silica nanoparticles will be affected by the environment of the polymer film in contrast to that in solution. To address these challenges, a well-defined polymer matrix with controlled surface characteristics is necessary.

Here, we explore the combination of top-down and bottom-up approaches to control the silica deposition on a photopatterned hydrogel substrate grafted with polyamine brushes. The microscopic shape of silica films will be determined by the hydrogel pattern, whereas the morphology of silica nanoparticles will be controlled by the characteristics of polyamine brushes (e.g., chemistry, composition, molecular weight, architecture, thickness, and grafting density). Because polyamines are not compatible with conventional photolithographic processes that involve generating photoacids upon exposure to light, we first patterned a hydrogel film from poly(2-hydroxyethyl methacrylate-*co*-acrylic acid, PHEMA-*co*-PAA) followed by tethering poly(ethyleneimine) (PEI) (both linear and branched) with different molecular weights (MW = 600−10 000 g/mol) to the film through a grafting process to direct the deposition of silica nanoparticles at room temperature and mild pH (∼5). The deposition was found to be site-specific, and the film thickness and morphology of the SiO_2 nanoparticles were controlled by PEI molecular weight and exposure time to the silicic acid precursor. FT-IR results suggested that PEI attacked the ethyl ester groups on PHEMA in the swollen PHEMA-*co*-PAA film, resulting in complete penetration of PEI chains and deposition of silica nanoparticles throughout the film. After pyrolysis at 500 °C, a faithful SiO_2 replica of the patterned polymer template was obtained. We believe the synthetic route we described here could be extended to the synthesis and patterning of a wide range of inorganic oxides, including TiO_2, ZnO, and V_2O_5, with controlled hierarchical organization.

Materials and Methods

Unless noted, all chemicals were purchased from Aldrich, Inc., and used as received.

Synthesis of Poly(2-hydroxyethyl methacrylate-*co*-acrylic acid), (PHEMA-*co*-PAA). The PHEMA-*co*-PAA random copolymers were synthesized using 2,2′-*azo*-bis(2-methylpropionitrile) (AIBN) as a radical initiator. For example, 9.34 mL of HEMA (10.00 g, 0.077 mol) and 1.32 mL of AA (1.38 g, 0.019 mol) were dissolved in 250 mL of tetrahydrofuran (THF, 99.9%) under N_2 in a 500 mL three-necked round-bottom flask fitted with a thermometer, a condenser, and a septum. AIBN (0.34 g, 3.0 wt %) was added to the solution after 20 min of stirring, and the reaction temperature was raised to 60 °C for 18 h. Excess THF was evaporated with rotary distillation and the product was precipitated with diethyl ether. After the polymer was washed with two additional cycles of dissolution in methanol and precipitation in diethyl ether, the resulting white powder was dried under a vacuum at room temperature, with an overall yield of 6.91 g (60.7%). The chemical compositions of the polymers were calculated using ^{1}HNMR (δ, ppm in CD_3OD) from the hydroxyethyl protons in HEMA (HOC$\boldsymbol{H}_2$C$\boldsymbol{H}_2$, 4.05, 2H, and 3.78, 2H, respectively) and the aliphatic backbone protons in HEMA (C$\boldsymbol{H}_2$CC$\boldsymbol{H}_3$, 2.76−0.95, 5H) and AA (C$\boldsymbol{H}_2$C$\boldsymbol{H}$, 2.76−0.95, 3H). The normalized molar ratio of HEMA:AA is 87:13, close to the 80:20 mol/mol feed ratio. Because the copolymers are not readily soluble in THF, their molecular weight and polydispersity were not measured by gel permeation chromatography (GPC).

Photo-Cross-Linking of PHEMA-*co*-PAA Films. Photo-cross-linked films were prepared following the procedure described previously.[28] Briefly, 30 wt % PHEMA-*co*-PAA, 10 wt % tetrakis-(methoxymethyl)glycouracil (TMMG, Powderlink 1174 Resin, Cytec Industries) as cross-linker, and 3 wt % Cyracure UVI-6976 (Dow Chemical) as photoacid generator were dissolved in 1.84 mL of dimethyl sulfoxide (DMSO). The solution was spin-cast on Si wafers at 3000 RPM for 30 s. The film was soft baked at 65 °C for 2 min followed by UV exposure (B-100AP, Blak-Ray) at an intensity of 7 mW/cm^2 for 300 s. After a postexposure bake at 65 °C for 5 min, the film was developed in methanol to dissolve the unexposed regions.

Poly(ethyleneimine) (PEI) Tethering on Cross-Linked PHEMA-*co*-PAA Films. PEI of different molecular weights, MW = 600 (branched), 1800 (branched), 2500 (linear), and 10 000 (branched) (Polysciences, Inc.) were used. Branched PEI has a primary:secondary:tertiary amine ratio of 1:2:1 with randomly distributed branching sites and a general backbone of $(CH_2CH_2NH)_x$. Linear PEI possesses only secondary amines in the backbone but terminated with primary amine chain ends. The crosslinked PHEMA-co-PAA film (2.5 × 2.5 cm^2) were soaked in a PEI/ethanol solution (0.5 mg/mL) for 12−15 h at room temperature, followed by rinses with ethanol and 10 mM HCl to remove physically absorbed PEI from the hydrogel template.

Fluorescein Isothiocyanate (FITC) Labeling. PEI-tethered PHEMA-*co*-PAA films were soaked in a FITC (from Invitrogen)/ethanol solution (1 mg/mL) for 12−15 h and washed with fresh ethanol to remove any nonspecifically bound FITC.

Silica Deposition on Cross-Linked PHEMA-*co*-PAA/PEI Films. The PEI-tethered hydrogel templates were treated with 0.5 M silicic acid, $Si(OH)_4$, in a 1 M phosphate−citrate buffer solution

(21) Knecht, M. R.; Wright, D. W. *Langmuir* **2004**, *20*, 4728.
(22) Jin, R.-H.; Yuan, J.-J. *Macromol. Chem. Phys.* **2005**, *206*, 2160.
(23) Yuan, J.-J.; Jin, R.-H. *Adv. Mater.* **2005**, *17*, 885.
(24) Brott, L. L.; Naik, R. R.; Pikas, D. J.; Kirkpatrick, S. M.; Tomlin, D. W.; Whitlock, P. W.; Clarson, S. J.; Stone, M. O. *Nature* **2001**, *413*, 291.
(25) Xu, M.; Gratson, G. M.; Duoss, E. B.; Shepherd, R. F.; Lewis, J. A. *Soft Matter* **2006**, *2*, 205.
(26) Glawe, D. D.; Rodriguez, F.; Stone, M. O.; Naik, R. R. *Langmuir* **2005**, *21*, 717.
(27) Kim, D. J.; Lee, K.-B.; Chi, Y. S.; Kim, W.-J.; Paik, H.-J.; Choi, I. S. *Langmuir* **2004**, *20*, 7904.
(28) Yang, S.; Ford, J.; Ruengruglikit, C.; Huang, Q.; Aizenberg, J. *J. Mater. Chem.* **2005**, *15*, 4200.

Scheme 1 Schematic Illustration of (A) Photocrosslinking of PHEMA-*co*-PAA Film in the Presence of PAG and TMMG, and (B) Grafting PEI to Cross-Linked PHEMA-*co*-PAA through an S_{N2} Reaction with the Ethyl Ester on PHEMA

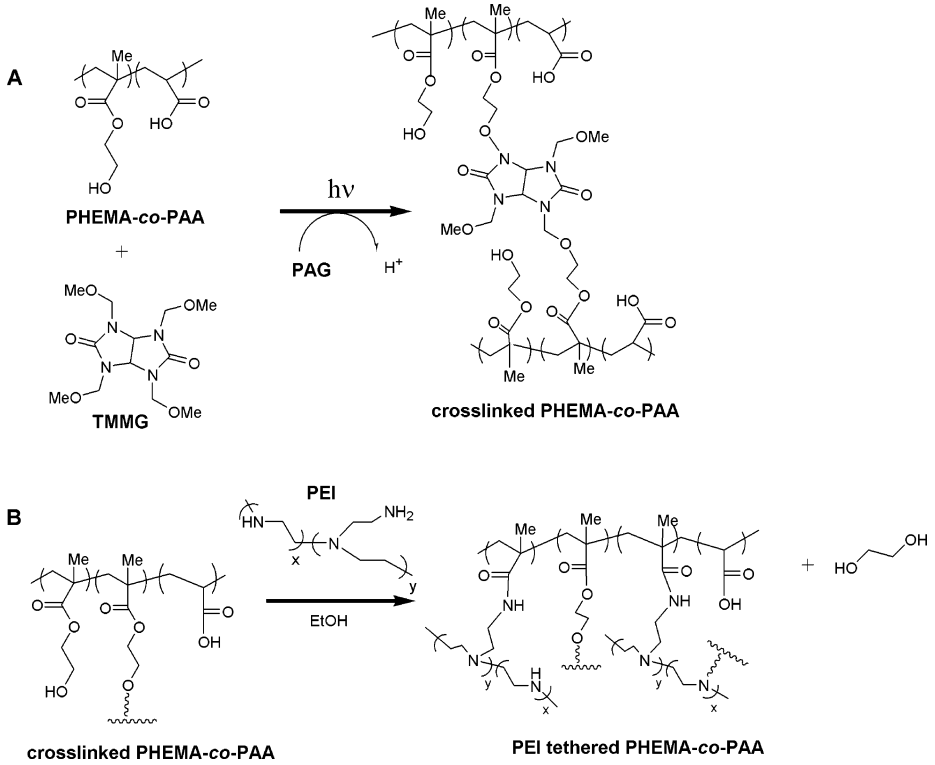

(pH 5) for 5−60 min. The silicic acid solution was prepared by hydrolyzing tetramethoxysilane (TMOS) in 1 mM HCl for 10 min. After treatment, the PEI-tethered films were washed with methanol three times and air-dried. The silica/polymer films were then placed in a cubic muffle furnace in an air environment and pyrolyzed at 500 °C for 3 h. The temperature was raised to 500 °C at a heating rate of 10 °C/min and cooled down slowly.

Characterization. The patterned polymer templates and the morphology of silica nanoparticles deposited within the films were imaged by scanning electron microscopy (SEM, FEI Strata DB235), and optical and fluorescence microscopies (Olympus BX60). Profilometry (Alpha Step) was used to measure the film thickness, where the polymer was patterned into 180 μm × 25 000 μm lines. The values were averaged over 20 data points in the central 100 μm of 5 separate lines. FT-IR spectra (128 scans) were obtained with a Nicolet Nexus 470 equipped with a MCT−B detector.

Results and Discussion

To study the directed deposition of silica on patterned polymer films, we should consider several design factors for the underlying polymer template, including (1) photopatternablility and resolution, (2) adhesion to the substrate (e.g., silicon wafer and glass slides), (3) functional groups for coupling polyamines, (4) uniformity and density of polyamine groups across the polymer template, and (5) thermal and mechanical stability along with swellability in solvent.

Poly(2-hydroxyethyl methacrylate) (PHEMA) has been widely studied as a synthetic hydrogel because of its biocompatibility and high transparency. Recently, radically polymerized PHEMA hydrogels have been studied as scaffolds to direct the growth of hydroxyapatite for tissue engineering.[29,30] By copolymerizing HEMA with various monomers, we can tailor the film surface functionalities, resist performance, and thermal and mechanical properties. Previously, we have designed poly(2-hydroxyethyl methacrylate-*co*-methyl methacrylate) (PHEMA-*co*-PMMA) copolymers as chemically amplified negative-tone resists,[28] which can be photo-cross-linked by photoacid generators (PAGs) and external crosslinkers, such as TMMG, as shown in Scheme 1A.[28] Here, we copolymerized HEMA with acrylic acid (AA), expecting that AA groups would provide coupling sites to covalently graft polyamines.

Polyethyleneimine (PEI) has a relatively high density of amino groups and can be dissolved in a wide range of solvents. Therefore, it was chosen as the polyamine of interest for grafting to the photopatterned PHEMA-*co*-PAA films. It is known that carboxylic acid and amino groups can form amide bonds through a dicyclohexyl carbodiimide (DCC)- and *N*-hydroxysuccinimide (NHS)-mediated reaction.[31] PEI with different molecular weights and architectures (linear vs branched) are readily available commercially and have been used to catalyze silica deposition in solution.[19]

The incorporation of acrylic acid groups into the polymer backbone, however, affected the baking temperature and the solubility of the photoresist; unexposed films heated at 90 °C became cross-linked because of the additional protons introduced by AA. AA also made the films pH sensitive. The hydrogel film swelled and delaminated from the Si wafer when exposed to solutions with pH >5. Further, the postexposure (PEB) temperature affected the hydrogel film cross-link density, which in turn influenced the PEI grafting efficiency along the film depth and the thickness of silica

(29) Song, J.; Saiz, E.; Bertozzi, C. R. *J. Am. Chem. Soc.* **2003**, *125* (5), 1236.
(30) Song, J.; Malathong, V.; Bertozzi, C. R. *J. Am. Chem. Soc.* **2005**, *127*, 3366.
(31) Grabarek, J.; Gergely, J. *Anal. Biochem.* **1990**, *185*, 131.

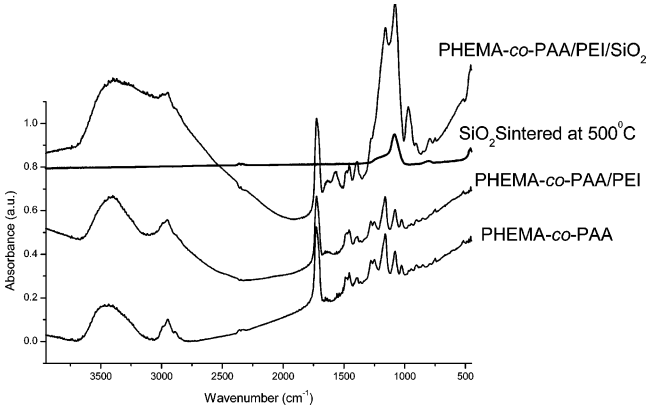

Figure 1. FT-IR spectra of PHEMA-*co*-PAA/PEI/SiO_2 composite films at different tethering and thermal treatment stages.

deposition. Thus, the HEMA:AA molar ratio was kept above 5:1 and the PEB temperature at 65 °C. To minimize unwanted film lift-off due to pH change during PEI grafting, we used ethanol or methylene chloride as solvent.

To characterize the grafting efficiency and study mechanism of the grafting reaction, we compared the FT-IR spectra of PHEMA-*co*-PAA before and after coupling of PEI. We observed an increases in peak absorption at 3400 cm^{-1} (ν_{N-H}) and 3000 cm^{-1} (ν_{C-H}), a slight shift at 1720 cm^{-1} ($\nu_{C=O}$), and an increase at 1650 cm^{-1} ($\nu_{C=O}$ of amide I band, ν_{N-H}) and 1570 cm^{-1} ($\nu_{C=OO^-}$) (Figure 1). These changes suggest formation of amide bonds between PEI and PHEMA-*co*-PAA, deprotonated COO^- groups, and physical absorption of PEI on PAA through electrostatic interaction. Because the latter interaction was relatively weak, the physically absorbed PEI was easily washed off from the hydrogel template with 10 mM HCl. However, when soaking the cross-linked PHEMA-*co*-PAA films in a PEI/ethanol bath for 16 h without DCC/NHS, similar FT-IR results were obtained, implying that HEMA groups, not AA, were mainly responsible for PEI coupling. Song et al.[29,30] have suggested that the ethyl esters on PHEMA can be thermally decomposed and hydrolyzed, converting PHEMA to poly(methacrylic acid) (PMAA). We suspect that in our system, the primary amines in PEI undergo S_{N2} substitution by attacking the ethyl ester groups of PHEMA (Scheme 1b). Because the PHEMA is the major component in the hydrogel film (PHEMA/PAA= 87:13 mol %), PEI/PHEMA reaction dominates over the PEI/PAA coupling, and FT-IR remained the same with or without DCC/NHS. In addition, PEI may act as a cross-linker that further cross-links the HEMA−AA matrix to a certain degree because there are many available amine groups to form amides with the acrylates. In contrast to the urea-mediated thermal decomposition of PHEMA, which requires urea as catalyst, elevated temperature (90−95 °C), and high pH (~8), our reaction took place at room temperature, and the ethyl ester substitution seems to occur throughout the film as opposed to only on the surface as reported by Song et al.[29,30] Evidence of PEI throughout the film will be discussed in detail later with silica deposition. To confirm the presence of PEI on the PHEMA copolymer films, we labeled the PEI-tethered films with fluorescein isothiocyanate (FITC). As seen in Figure 2, fluorescence microscopy revealed enhanced

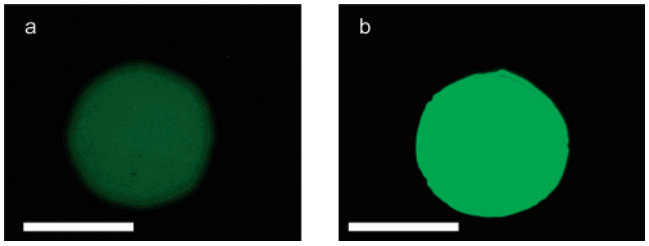

Figure 2. Fluorescence microscopy images of FITC labeled films: (a) PHEMA-*co*-PAA and (b) PEI-tethered PHEMA-*co*-PAA. Scale bar: 100 μm.

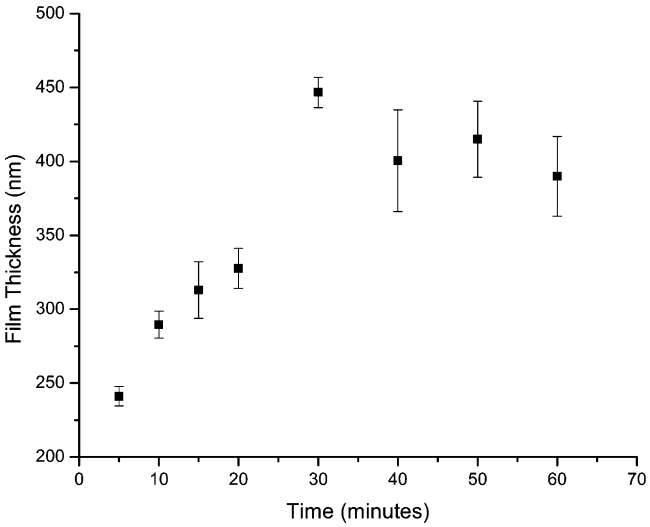

Figure 3. Film thickness of PHEMA-*co*-PAA/PEI (MW = 10 000) treated with $Si(OH)_4$ for different reaction times, followed by pyrolysis at 500 °C for 3 h.

fluorescence intensity and uniform grafting of PEI across the pattern.

After PEI was tethered to the PHEMA-*co*-PAA template, the film was exposed to a buffered (pH 5) silicic acid solution. Because the polymer film would swell and delaminate from the substrate at pH >5, the silicification reaction was carried out at pH 5. At this pH value, no autocondensation or gelation of the silicic acid solution was observed within 60 min. Thickness measurements of the pyrolyzed SiO_2 deposited in PHEMA-*co*-PAA/PEI (MW = 10 000) showed that SiO_2 nanoparticles were readily deposited on to the polymer template within 5 min and continued up to 30 min, after which the SiO_2 condensation reaction was saturated (Figure 3). In later studies of the size and morphology of silica nanoparticles grown on PHEMA templates, we treated the films with silicic acid at pH 5 for 30 min.

At pH 5, the amino groups of PEI were completely protonated. In aqueous solutions, $Si(OH)_4$ forms a number of negatively charged species, which electrostatically aggregate around the PEI chains.[11] Further reaction with $Si(OH)_4$ led to the condensation of Si−O−Si networks within the PHEMA-*co*-PAA/PEI template. The FT-IR spectra of the SiO_2−polymer composite films revealed large increases at 3300 cm^{-1} (ν_{O-H}), 1570 cm^{-1} ($\nu_{C=OO^-}$), and 1100, 960, and 460 cm^{-1} (ν_{Si-O}) (Figure 1). The polymer patterns were completely decomposed after pyrolysis at 500 °C for 3 h, confirmed by the disappearance of the characteristic absorbance peaks of the PHEMA-*co*-PAA and PEI in the FT-IR

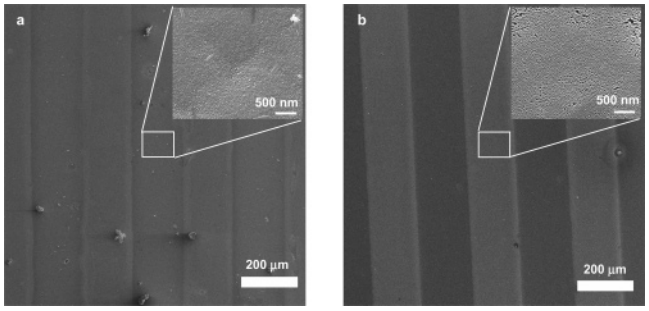

Figure 4. SEM images of photopatterned PHEMA-*co*-PAA/PEI (MW = 10 000)/SiO_2 films (a) before and (b) after pyrolysis at 500 °C for 3 h. Scale bar: 200 μm.

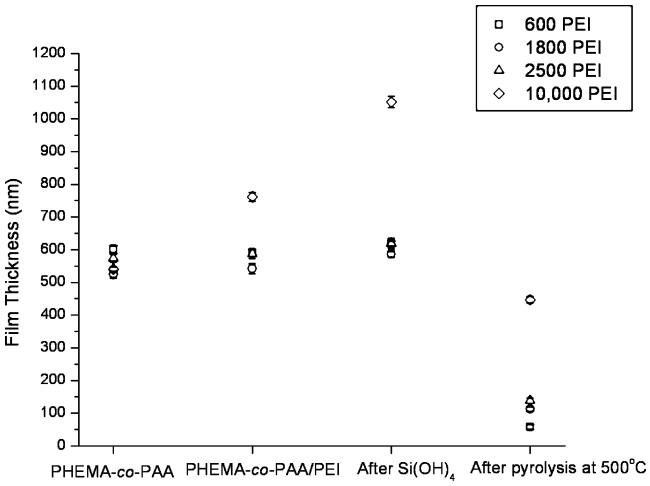

Figure 5. Thickness of PEI tethered films with different molecular weights at different treatment stages.

spectrum, leaving only the peaks of Si−O−Si bonds (Figure 1). Scanning electron microscopy (SEM) images of the crosslinked PHEMA-*co*-PAA films with simple line patterns (line width and separation of 180 μm) before and after silica deposition/pyrolysis implies that the deposition of silica nanoparticles is site-specific, that is, silica was deposited only in the patterned regions (Figure 4). More interestingly, there is little change in the pattern size and shape, which makes our method attractive to pattern complex silica structures without sacrificing film integrity.

It has been suggested that the size and morphology of silica nanoparticles and their coverage on the polymer template could be affected by the molecular weight of polyamines and their chemical structures (primary vs secondary vs tertiary amines).[19] Here, we varied the molecular weight of PEI from 600, 1800, and 2500 to 10 000 g/mol. Except for the linear one with MW of 2500, all other PEIs were branched polymers with a primary:secondary:tertiary amine ratio of 1:2:1. When the PEI chains were short (MW = 600, 1800, and 2500 g/mol), little change in the overall film thickness was observed after PEI tethering, in contrast to an increase of ~200 nm for PEI with a MW of 10 000 (Figure 5). After exposure to silicic acid, a 50 nm thickness change was observed for the smaller PEI chains in comparison to a 300 nm increase for PEI of 10 000 g/mol. After the silica/polymer composites were pyrolyzed at 500 °C for 3 h, the overall film thicknesses ranged from 50 to 450 nm, increasing with PEI molecular weight (Figure 5). The relative surface coverage of silica also increased with molecular weight

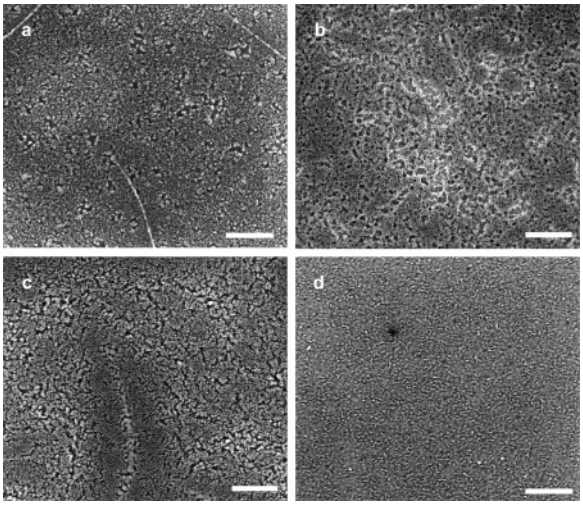

Figure 6. SEM images of silica nanoparticles deposited on PHEMA-*co*-PAA/PEI films with different PEI molecular weights: (a) MW = 600, (b) MW = 1800, (c) MW = 2500, and (d) MW = 10 000 g/mol, respectively. Scale bars: 500 nm. All PHEMA-*co*-PAA/PEI films were exposed to $Si(OH)_4$ at pH 5 for 30 min, followed by pyrolysis at 500 °C for 3 h.

(Figure 6). AFM images of the deposited silica films (Figure 7) show that the SiO_2 nanoparticles are nearly spherical and form a smooth film from low molecular weight PEIs (600 and 1800 g/mol). When the PEI molecular weight was increased beyond 2500 g/mol, the silica nanoparticles started to aggregate, and the particle size increased from 14 nm (PEI MW = 600 g/mol), to 17 nm (MW = 1800 g/mol), to ~25 nm (MW = 2500 and 10 000 g/mol), respectively. There was little difference in film thickness change (Figure 5) and morphology (Figure 6) of the silica deposited from branched and linear PEIs with similar molecular weights, 1800 and 2500 g/mol, respectively. The film surface roughness and nanoparticle size, however, were found to be dependent on PEI architecture (images b and c in Figure 7).

It is interesting to note that the original film pattern is maintained after silica deposition and pyrolysis (Figure 4). The question remained as to whether the silica nanoparticles were deposited only on the template surface, forming a shell, or throughout the film. To understand the silica deposition mechanism in our system, we compared a series of cross-sectional SEM images of the untreated PHEMA-*co*-PAA film, PHEMA-*co*-PAA/PEI/SiO_2 composite, and the pyrolyzed SiO_2 film (Figure 8). Figure 8b clearly shows that SiO_2 nanoparticles (20 to 50 nm in diameter) were deposited throughout the PHEMA-*co*-PAA/PEI template, and the formation of the SiO_2 particles within the template caused film expansion normal to the substrate. After the film was pyrolyzed, the SiO_2 film was densified with little change in particle size and morphology (Figure 8c). These results are consistent with the film thickness change measurement by profilometry (Figure 5). However, they are in sharp contrast to the crystal growth of hydroxyapatite on the urea-decomposed PHEMA hydrogel networks, where crystals were found to grow only on the surface of the poly(methacrylic acid) gels.[28]

The growth of silica nanoparticles within the film can be explained by two cooperative effects: (1) the attack of ethyl ester groups on PHEMA or acid groups on PAA by PEI effectively incorporates PEI chains within the film, and (2)

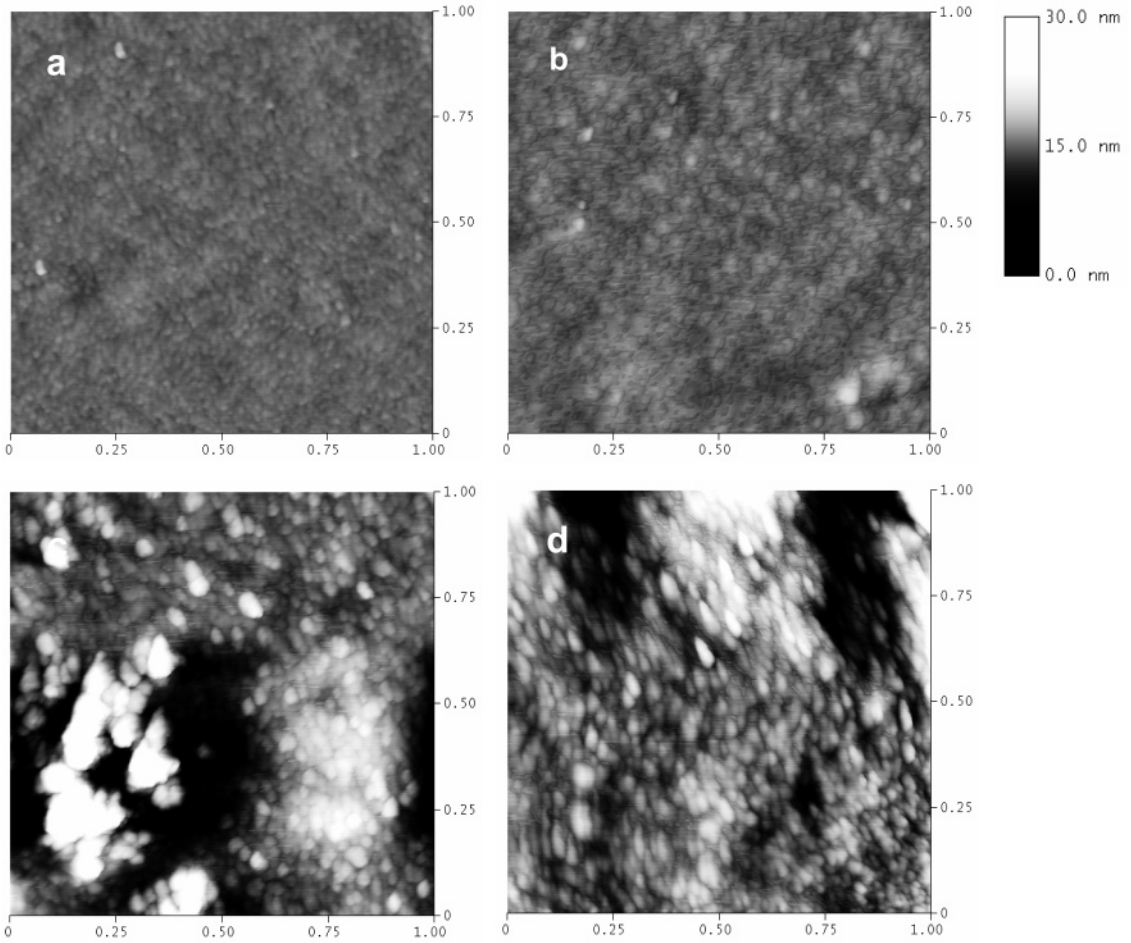

Figure 7. AFM images (1μm × 1μm) of silica nanoparticles deposited on PHEMA-*co*-PAA/PEI films with different PEI molecular weights. (a) MW = 600, (b) MW = 1800, (c) MW = 2500, and (d) MW = 10 000 g/mol, respectively. PHEMA-*co*-PAA/PEI was exposed to $Si(OH)_4$ at pH 5 for 30 min, followed by pyrolysis at 500 °C for 3 h.

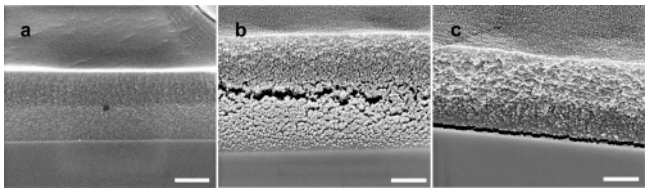

Figure 8. Cross-sectional SEM images of (a) PHEMA-*co*-PAA, (b) PHEMA-*co*-PAA/PEI (MW = 10 000) treated with $Si(OH)_4$ at pH 5 for 30 min, and (c) SiO_2 film after pyrolysis at 500 °C for 3 h. Scale bars: 500 nm.

swelling of the PHEMA-*co*-PAA film by PEI and/or ethanol leads to an overall increase in the volume of the hydrogel network. Because the cross-linked PHEMA-*co*-PAA is pH sensitive, addition of weakly basic PEI (pKa ~9) could cause film swelling, promoting the diffusion of PEI chains and the subsequent silica deposition through the film. To confirm the importance of the swellability of PHEMA-*co*-PAA network by PEI, we performed control experiments at different postexposure bake (PEB) temperatures and time. When baked at a higher temperature (≥90 °C) and/or longer baking time (>5 min), the PHEMA-*co*-PAA hydrogel films were highly densified, and the diffusion of PEI chains was limited. After silica deposition and pyrolysis, only ~20 nm of silica was measured, in contrast to ~400 nm of silica from those baked at 65 °C for 5 min.

Conclusions

We studied the directed deposition of silica on photopatterned PHEMA-*co*-PAA hydrogel films that were tethered with poly(ethyleneimine) (PEI) (both linear and branched) through a grafting approach, followed by a sol−gel reaction at room temperature and pH 5. The silica deposition was found to be site-specific (only on patterned hydrogel/PEI), and the film thickness and morphology of the SiO_2 nanoparticles could be controlled by PEI molecular weight and exposure time to $Si(OH)_4$. Our study suggested that PEI attacked the ethyl ester groups on PHEMA and swelled the PHEMA-*co*-PAA film, resulting in complete penetration of PEI chains and deposition of silica nanoparticles throughout the film. After pyrolysis at 500 °C, a faithful SiO_2 replica of the patterned polymer template was obtained. Our preliminary results suggest that the synthetic route we described here can be extended to the synthesis and patterning of a wide range of inorganic oxides, including TiO_2, ZnO, and V_2O_5, as well as to the assembly of non-oxide inorganic materials with controlled micro- and nanostructures.

Acknowledgment. We thank Seth Marder and Nils Kröger (Georgia Institute of Technology) for helpful discussion. This research is supported by the Office of Naval Research (ONR), Grant N00014-05-0303, and the National Science Foundation (NSF)/CAREER Grant DMR-0548070. S.Y. is thankful for the 3M Nontenured Faculty Grant.

CM071566Q